

**Au-induced atomic wires on stepped Ge(*hkk*) surfaces**

T. Wagner, J. Aulbach, J. Schäfer, and R. Claessen

*Physikalisches Institut and Röntgen Center for Complex Material Systems (RCCM),  
Universität Würzburg, Am Hubland, D-97074 Würzburg, Germany*

(Received 3 August 2018; published 17 December 2018)

Au adsorption on high-index Si surfaces is known to form quasi-one-dimensional surface reconstructions with interesting physical properties such as Rashba-split bands and ordered arrays of local magnetic moments. Here we report on a novel family of Au-induced chain systems, hosted on Ge(*hkk*) substrates. Our study includes Ge(553), Ge(557), and Ge(335) for both bare and Au-adsorbed surfaces, respectively. We employ scanning tunneling microscopy and low-energy electron diffraction to characterize the topography and the occurrence of superstructures. Stable bare surfaces with regularly distributed steps are found for the (553) and (335) orientations. For nominal Ge(557) substrates a refaceting to Ge(223) is observed. Addition of Au tends to promote a change in the surface index which creates Ge(221)-Au, Ge(557)-Au, and Ge(335)-Au surfaces. Their STM images show elements that are reminiscent of the well-understood Si(*hkk*)-Au surfaces but also reveal important differences.

DOI: [10.1103/PhysRevMaterials.2.123402](https://doi.org/10.1103/PhysRevMaterials.2.123402)**I. INTRODUCTION**

With modern devices getting smaller, the interest in the electronic properties of low-dimensional systems is strongly increasing, as electronic circuits may soon face quantum-mechanical effects when reaching the transition regime between three-dimensional (3D) and lower-dimensional behavior. Especially in one-dimensional (1D) systems, due to the strong confinement of the electrons, unusual phenomena can be observed, such as Peierls instabilities [1] or Tomonaga-Luttinger liquids [2]. In the latter case the quasiparticle picture of Landau's Fermi liquid theory breaks down, caused by the strong electron-electron interaction in 1D which allows only collective charge and spin excitations. In addition, spin ordering on surfaces has attracted strong interest for future spintronic applications [3], e.g., as spin-based memory device [4]. Both aspects have strongly promoted the investigation of electronic properties of 1D surface nanostructures on semiconductor surfaces. Based on substrates that are either planar, e.g., (001) or (111) oriented, or exhibit a stepped surface with high Miller indices, e.g., (*hkk*), they serve as ideal templates for metal atoms (e.g., Au, Ag, Pb) [5–9] to form self-assembled 1D structures.

Regarding high-index surface systems, the so-called *Si(hkk)-Au family* [6,10] is a prominent representative. All members show a Rashba-type spin-orbit splitting of their Au-induced surface bands [6,11] and some are known for forming a regular array of local magnetic moments at their Si honeycomb step edges, e.g., Si(553)-Au and Si(557)-Au [12–14]. The surfaces themselves consist of Au atoms adsorbed on a Si substrate whose surface orientation is tilted away from the planar (111) surface towards the [11-2] direction. This leads to the formation of regularly stepped surfaces with the terrace width depending on the miscut angle. The surfaces comprise (111) terraces separated by steps of single atomic height. Through thorough theoretical work using density functional

theory (DFT) and the comparison of simulated and experimental data from scanning tunneling microscopy (STM), atomic models for all known stable surface orientations, i.e., Si(553)-Au, Si(775)-Au, Si(335)-Au and Si(557)-Au, have been derived and are by now well established [6,15,16]. They consist of either a single or double Au strand, a graphenelike Si honeycomb (HC) at the step edge, and, in some cases, a Si adatom chain. Each Si atom at the HC step edge possesses one dangling bond which can be spin polarized if it is occupied by just a single electron. In case of Si(553)-Au two thirds of the dangling bond orbitals are fully occupied while one third is single occupied, imprinting a  $\times 3$  superstructure along the step edge [13].

Quasi-1D model systems based on self-assembled atomic wire growth on a semiconducting template provide the opportunity to vary either the substrate or adatom material, respectively, in order to create new model systems with modified electronic and structural properties. Exemplary, different metal atoms have already been used as adatoms on stepped Si(*hkk*) surfaces, e.g., Pb [17] or Ag [18], and the self-organization of metal atoms has also been used to achieve nanowire growth on planar Ge(001) surfaces [19,20].

In this study we extend the class of Si(*hkk*)-Au surfaces to stepped Ge(*hkk*) substrates. The small difference in the lattice constant of both group IV elements of 4.2% ( $a_{\text{Ge}} = 5.66 \text{ \AA}$ ,  $a_{\text{Si}} = 5.43 \text{ \AA}$ ) suggests similar growth conditions and the formation of stable Au-induced surface reconstructions. Differences, however, exist regarding the bonding characteristics of both substrates causing distinct reconstructions for their respective (111) surfaces after thermal treatment [21,22], a  $(7 \times 7)$  for Si and a  $c(2 \times 8)$  for Ge. In addition, the band gap of Ge (0.66 eV) is only half that of Si (1.12 eV), giving rise to a stronger electronic screening. These differences will necessarily have influence on the electronic properties of the surface, e.g., on the Coulomb interaction strength of potentially present dangling bonds. To compare our results on

Ge(*hkk*)-Au to those of other established surface systems, we use the stable (*hkk*) orientations of the Si(*hkk*)-Au family as reference.

## II. EXPERIMENTAL DETAILS

The Ge(*hkk*) samples used in this work are p-type Ge(553) and Ge(335) (B doped) and n-type Ge(557) (Sb doped). The *ex situ* preparation for all Ge(*hkk*) samples was identical and conducted in a laminar flow box in a clean room environment. The samples were cleaned in an ultrasonic bath with acetone, isopropanol, and methanol of highest purity for 2 min in each solvent, after the protective photoresist was removed with standard grade acetone. To avoid residual solvents the samples were blown off with dry nitrogen. The base pressure of the UHV chamber used for the *in situ* preparation was below  $5 \times 10^{-10}$  mbar. After degassing the samples, they were flashed several times up to 900 °C. Clean and well-ordered substrate surfaces have been achieved by several cycles of Ar<sup>+</sup> sputtering (partial pressure  $5 \times 10^{-5}$  mbar) with a subsequent thermal treatment. Au was evaporated by a standard e-beam evaporator for 2 min for each sample preparation. Images obtained by low-energy diffraction (LEED) are all taken at room temperature, STM images at 77 K.

## III. RESULTS AND DISCUSSION

### A. Ge(553) and refaceting to Ge(221)-Au

After substrate preparation the bare surface of Ge(553) shows spots of the  $(1 \times 1)$  unit cell of the unreconstructed Ge(111) surface [Fig. 1(a)] with each spot split into subspots. This splitting indicates the presence of regular steps on the sample surface [24]. The terrace width of  $(3.00 \pm 0.15)$  nm, as determined by the LEED spot spacings, corresponds to a Ge(553) surface with steps of double atomic height. After depositing Au onto this clean Ge(553) surface the observed LEED pattern shows spots of a surface with regularly distributed steps [Fig. 1(b)] indicated by main spot rows. In addition, spots of a  $(\sqrt{3} \times \sqrt{3})_{111}$  surface reconstruction, with respect to the  $(1 \times 1)$  unit cell of the (111) substrate as indicated by the index, are visible. An STM topographic image shows two different surface reconstructions on the Au-induced surface [Fig. 1(c)]. On one hand, there are up to 35 nm wide areas with a regular chainlike structure. The interchain distance of  $(1.2 \pm 0.1)$  nm corresponds to the terrace width of a stepped (221) surface. On the other hand, planar domains can be found in between these stepped areas separated by straight boundaries oriented along the  $[1\bar{1}0]$  direction parallel to the chainlike structure. The respective surface normal vectors of these differently reconstructed domains (determined with STM, not shown here) differ by an angle of  $16.2^\circ$ . In combination with the  $(\sqrt{3} \times \sqrt{3})_{111}$  spots observed in LEED, this leads to the conclusion that the planar domains comprise Ge(111)-Au surfaces. For Ge(111), the  $(\sqrt{3} \times \sqrt{3})$ -Au reconstruction has first been observed by Margoninski *et al.* [25] and was studied in detail by some of the present authors [26]. Offering Au atoms to the (553) substrate therefore evokes a refaceting into alternating domains of Ge(221)-Au and Ge(111)-Au. Such an adsorbate-induced refaceting is known to exist for many different surfaces [27] and has

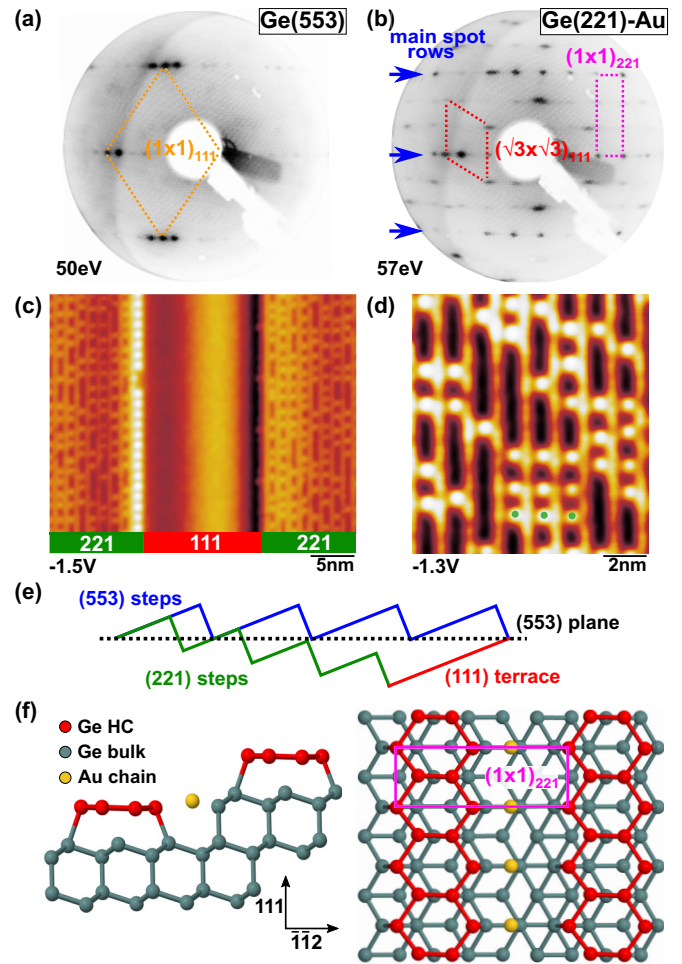


FIG. 1. (a) LEED image of the clean Ge(553) surface with the  $(1 \times 1)$  unit cell of the unreconstructed Ge(111) surface showing split main spots. (b) After Au evaporation, LEED shows intense spot rows of a regularly stepped surface and spots of a  $(\sqrt{3} \times \sqrt{3})_{111}$  surface. The reconstructed Au-induced surface itself shows a rectangular  $(1 \times 1)_{221}$  unit cell. (c) STM topography image (50 pA) shows a refaceted surface with alternating Ge(221)-Au and Ge(111)-Au domains. (d) Detailed STM image (50 pA) of chainlike features on the Ge(221) surface with bright protrusions in between showing a horizontal alignment (green dots). (e) Schematic of the refaceting of the Ge(553) surface to the Au-covered (221) and (111) oriented domains. (f) Side and top view of a structural atomic model based on the atomic models of the Ge(111)-M [23] and Si(*hkk*)-Au surfaces [6]. In contrast to all Si(*hkk*)-Au surface reconstructions the  $(1 \times 1)_{221}$  unit cell has a rectangular shape.

especially also been observed for Pb on Si(557) [28]. The coexistence of both surface orientations after the Au-induced refaceting of the Ge(553) substrate is inevitable in order to compensate the miscut of  $3.5^\circ$  between the (553) and (221) surface as schematically depicted in Fig. 1(e).

Figure 1(d) provides a detailed view of the Ge(221)-Au topography with STM. The image taken at a tunneling bias of  $-1.3$  V is dominated by nearly homogeneous high-intensity channels running along the step edge direction with bright protrusions between them. The protrusions are separated by multiples of half the surface lattice constant ( $a_0 = 4.00 \text{ \AA}$ )

with a minimum distance of  $3a_0$ . As there is no theoretical calculation for an atomic structure model of this surface, a clear assignment of the observed topographic features to structural features of an atomic model, e.g., honeycombs or adatoms, cannot be made. Nevertheless, compared to the known  $\text{Si}(hkk)\text{-Au}$  surfaces, the linear feature running along the step edge direction can most probably be attributed to the step edge as this is the most prominent and most regular topographic feature on all known  $\text{Si}(hkk)\text{-Au}$  surfaces. Whether the Ge step edge is composed by a HC structure or not cannot be concluded from STM, but the energetic stability of this structural motif is known from  $\text{Ge}(111)\text{-M}$  surfaces (M: Li, Na, K, Ag) [23,29]. The bright protrusions between the high intensity channels might probably arise from adatoms lying on top of the terraces. Based on this educated guess, we propose the atomic structure depicted in Fig. 1(f), which in turn is derived from the structure models of  $\text{Ge}(111)\text{-M}$  [23] and the related  $\text{Si}(hkk)\text{-Au}$  family [6]. It features a Ge HC step edge with a neighboring Au chain. In contrast to the atomic models of  $\text{Si}(hkk)\text{-Au}$ , there is no shift of  $0.5a_0$  between the HCs of neighboring step edges. This is attributed to the atomic structure of the underlying substrate which intrinsically prevents a registry shift of the step edges for the terrace width of a stepped  $\text{Ge}(221)$  surface. Indeed, the lateral registry of the proposed model is in line with our LEED and STM observations. The LEED image [Fig. 1(b)] does not show a shift between adjacent main spot rows by half of the intrarow distance. This results in a rectangular  $(1 \times 1)_{221}$  unit cell [purple rectangle in Fig. 1(b)] instead of the rhombohedral unit cell known from all other  $\text{Ge/Si}(hkk)\text{-Au}$  reconstructions. The ‘missing’ lateral shift is also apparent in STM in the horizontal alignment of protrusions of neighboring terraces [green dots in Fig. 1(e)]. As the nature of the (disordered) bright protrusions in STM cannot be determined, they are not included in this simple atomic model.

## B. $\text{Ge}(557)$ and $\text{Ge}(557)\text{-Au}$

### 1. Plain $\text{Ge}(557)$ substrate refaceting to $\text{Ge}(223)$

The surface quality of the  $\text{Ge}(557)$  substrate could remarkably be enhanced by adding a long thermal treatment up to  $700^\circ\text{C}$  ( $\geq 30$  min) at the end of the substrate preparation. This is in analogy to the enhanced ordering of the bare  $\text{Si}(553)$  surface after a similar long-term thermal treatment as reported by Kopciuszynski *et al.* [30]. As for the  $\text{Ge}(553)$  surface, LEED shows the formation of a regularly stepped surface with split up main spots of the  $(1 \times 1)_{111}$  unit cell, see Fig. 2(a). Additional spots in between the main spot rows indicate a  $\times 5$  periodic superstructure with respect to the surface lattice constant  $a_0$  along the direction parallel to the step edge. These spots are well defined and not smeared out to streaks, indicating that the superstructures of neighboring chains have a fixed registry shift to each other [31]. In STM, regularly stepped areas up to 30 nm in width can be found, confined by step bunches of the substrate and covered with  $(3.31 \pm 0.07)$  nm wide terraces. This terrace width does not correspond to  $\text{Ge}(557)$  but rather to  $\text{Ge}(223)$  with steps of double atomic height ( $d_{223} = 3.29$  nm).

In general, a refaceting of the bare substrate is rather unusual for  $\text{Ge}(hkk)$  or  $\text{Si}(hkk)$ . One exception is  $\text{Si}(557)$ .

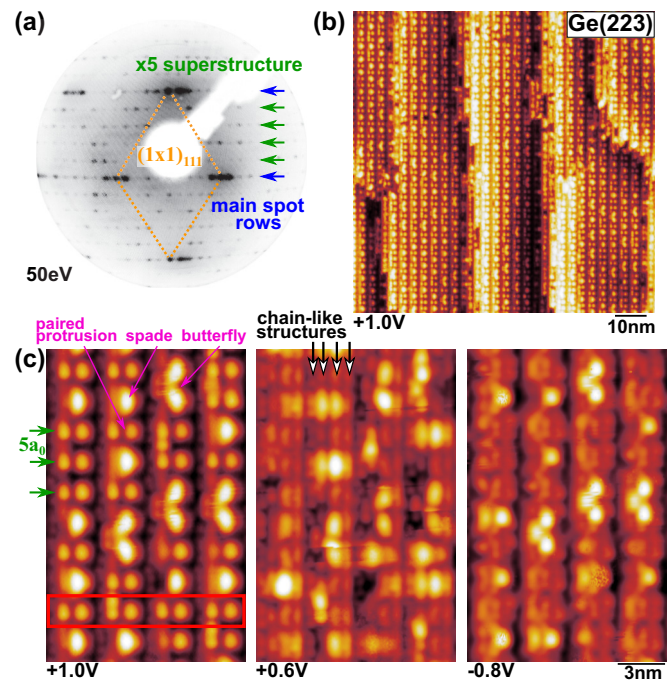


FIG. 2. (a) LEED and (b) STM (50 pA) images of the clean  $\text{Ge}(557)$  substrate show the formation of a  $\text{Ge}(223)$  surface with a  $\times 5$  superstructure along the step edges. (c) An STM bias series of a small surface area without major defects in the surface reconstruction reveals four chainlike features per  $\text{Ge}(223)$  terrace (see black/white arrows). Three different shapes of topographic features can be distinguished: (i) paired protrusions, (ii) a spadelike shape, and (iii) a butterflylike shape. The paired protrusions (i) are not only arranged in a regular  $\times 5$  superstructure along a single terrace but also order perpendicular to the step edge direction with the paired protrusions located on neighboring terraces (see red rectangle).

Here, different preparation procedures yield various stepped surface orientations, see Ref. [32] (and references therein). In particular, a refaceting to a  $\text{Si}(223)$  surface with steps of triple atomic height has been observed in case the direct current direction during the annealing procedure was orientated perpendicular to the step edge direction [33]. This was also the case for the  $\text{Ge}(557)$  substrate studied in this work. The refaceting to  $\text{Ge}(223)$  was observed for all different preparation parameters and therefore implies that the bare  $\text{Ge}(557)$  surface is unstable, at least for a heating current direction perpendicular to the step edges.

Detailed constant current STM images for varying tunneling biases show a well-ordered surface reconstruction, see Fig. 2(b), consisting of three different topographic features (most prominent at  $+1.0$  V): (i) paired protrusions (orientated perpendicular to the step edge direction), (ii) spadelike protrusions, and (iii) butterflylike features. The paired protrusions (i) intersect the terrace reconstruction in multiples of five times the surface lattice constant  $a_0$ , therefore causing the  $\times 5$  superstructure of Fig. 2(a). Their additional interterrace ordering [highlighted with the red box in Fig. 2(c)] is responsible for the well defined spots making up the superstructure observed with LEED. At a lower tunneling bias ( $U = +0.6$  V) four different chainlike structures can be distinguished

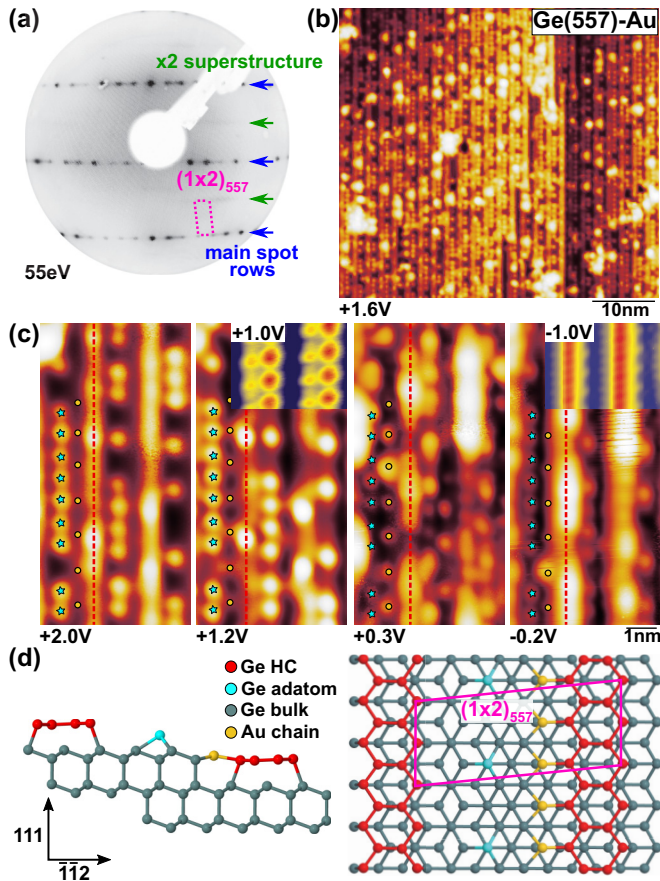


FIG. 3. (a) LEED pattern of the regularly stepped Ge(557)-Au surface with main spot rows and a streak of a  $\times 2$  superstructure along the step edge direction. (b) In STM, areas with regularly distributed Ge(557)-Au steps show many defects and adatoms. (c) A bias series of a small surface area reveals three chainlike structures per terrace: (cyan stars) pearl-like chain with  $\times 2$  superstructure, (yellow dots) pearl-like chain with  $\times 3$  superstructure, (red dashed line) irregular, cloudy chain. Small insets: STM images of the Si(557)-Au surface from Sauter *et al.* [35], also taken at 77 K, bear great resemblance to the Ge(557)-Au surface. (d) Atomic model of Ge(557)-Au with a  $(1 \times 2)_{557}$  unit cell in side and top view adapted from the Si( $h$ hk)-Au model from Crain *et al.* [6].

(indicated by black/white arrows) forming the reconstruction of a single terrace. In the occupied states, features keep their shape except the paired protrusions which become less prominent and are blurred out.

## 2. Au evaporation

Evaporating Au onto the Ge(223) surface results in the formation of two different surface orientations depending on the offered Au amount. For a small Au coverage,  $(2.1 \pm 0.2)$  nm wide terraces suggest the formation of a Ge(557)-Au surface (see Fig. 3). For larger Au amounts, LEED shows spots corresponding to a Ge(335)-Au surface as well as additional intensities caused by a  $(\sqrt{3} \times \sqrt{3})_{111}$  reconstruction (not shown here). The occurrence of the  $(\sqrt{3} \times \sqrt{3})$  spots indicates the existence of Ge(111)-Au domains which compensate the miscut between the Ge(557) substrate and the Ge(335)-Au

surface, in analogy to the refaceting of the Ge(553) substrate in Sec. III A. This coverage-dependent behavior of the surface reconstruction is also known for the related Si(557)-Au surface [34].

Here, we take a closer look at the Ge(557)-Au surface and defer the Ge(335)-Au reconstruction to the next section, where it is discussed in conjunction with its ‘native’ Ge(335) substrate. An investigation by LEED shows the main spot rows of a regularly stepped (557) surface together with the streak of a  $\times 2$  superstructure oriented parallel to the step edges [see Fig. 3(a)]. The LEED pattern therefore implies a  $(1 \times 2)_{557}$  surface unit cell. STM images reveal large Ge(557)-Au areas up to 50 nm in width with regularly distributed steps [see Fig. 3(b)]. Each terrace thereby shows a periodic surface reconstruction parallel to the step edge, which is, however, interrupted by many adsorbates and defects. Nevertheless, three different chainlike features can be found for each Ge(557)-Au terrace [see Fig. 3(b)]: (i) a pronounced  $\times 2$  superstructure (cyan stars) which is most prominent for high positive tunneling biases, (ii) a  $\times 3$  superstructure (yellow dots) which is visible at a tunneling bias of +0.3 V, and (iii) a smeared out, cloudlike shaped feature (red dashed line).

The lack of a structural model for the Ge(557)-Au surface hinders a clear interpretation of origin of the observed superstructures. However, STM images bear resemblance to the STM images of the well-understood Si(557)-Au surface. Sauter *et al.* [35] also observed a cloudy chainlike feature in the occupied states on the Si(557)-Au surface as well as a pronounced  $\times 2$  superstructure in the unoccupied states [see insets in Fig. 3(c)]. The first feature was assigned to the Si step edge while the latter is caused by a Si adatom chain [36,37]. Their resemblance in STM suggests that an atomic structure model for the Ge(557)-Au surface can most probably be based on that of the Si(557)-Au surface. An atomic model of Ge(557)-Au, adapted from the Si(557)-Au model of Crain *et al.* [6], is shown in Fig. 3(d). The model comprises Ge steps of single atomic height with Ge HC step edges, a single strand of Au atoms and an adatom chain with a twofold periodicity. Due to this superstructure, a  $(1 \times 2)_{557}$  unit cell arises which is compatible with the LEED pattern of Fig. 3(a). Assuming the proposed model is correct, the observed  $\times 3$  superstructure (yellow dots) would be the signature of the Au chain. The fact that this superstructure is apparent in STM but not in LEED images suggests the occurrence of a temperature-dependent phase transition in the temperature range between RT (LEED) and 77 K (STM). This transition could for example be a Peierls instability or a structural transition driven by electron-phonon coupling. In analogy, a metal-insulator transition in the same temperature range was found on Si(557)-Au [35,38,39] which is not fully understood until now. Without DFT total energy calculations, this model remains only a suggestion based on the known Si(557)-Au atomic structure due to the similarities in the topographic STM images in both occupied and unoccupied states.

## C. Ge(335) and Ge(335)-Au

In the above case, the Ge(335) areas resulted from the refaceting of a Ge(557) substrate. However, it can also be directly generated from a pre-cut Ge(335) substrate, thereby

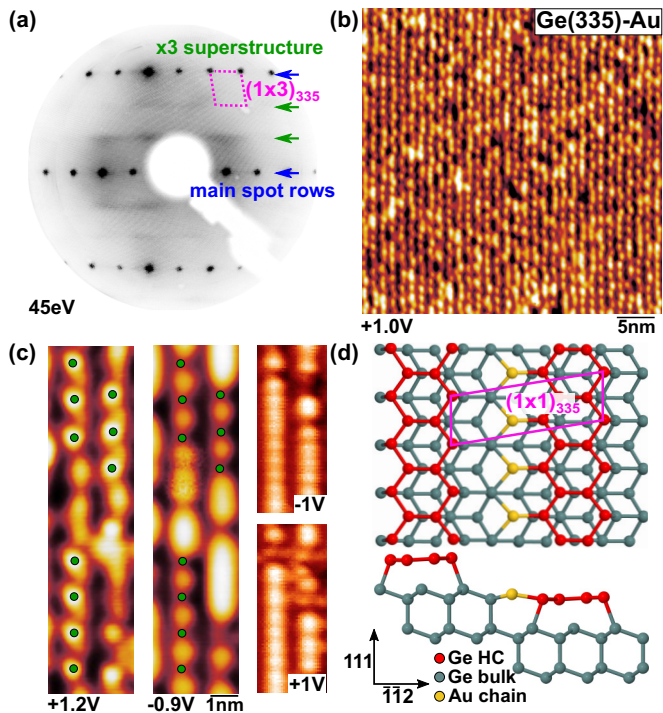


FIG. 4. (a) LEED and (b) STM (50 pA) image of the Ge(335)-Au surface. Besides the main spot rows, the LEED pattern shows streaks of a  $\times 3$  superstructure. In STM, large Ge(335)-Au areas with a regular step array up to 100 nm in width can be observed. (c) Detailed STM images of the Ge(335)-Au surface (left side) reveal small patches with a  $\times 3$  superstructure along the step edge direction (green dots). The intensities invert between images of the occupied and unoccupied states, similar to the Si HC step edge of the Si(335)-Au surface (right side) [40]. (d) Atomic structure model of Ge(335)-Au based on the Si(*hkk*)-Au atomic model, proposed by Crain *et al.* [6], overlaid with the corresponding  $(1 \times 1)_{335}$  unit cell.

avoiding defects caused by the refaceting. According to LEED images (not shown here), varying the parameters for the *in situ* substrate preparation leads to Ge(335) steps of either double or triple atomic height with terrace widths of  $(2.7 \pm 0.3)$  nm and  $(3.9 \pm 0.3)$  nm, respectively. Evaporating Au onto the clean substrate induces a surface with  $(1.3 \pm 0.1)$  nm wide Ge(335) terraces separated by steps of single atomic height. The LEED pattern [see Fig. 4(a)] suggests a  $(1 \times 3)_{335}$  unit cell of the surface due to streaks of a  $\times 3$  superstructure between adjacent main spot rows. The Au amount needed for a homogeneous sample of Ge(335)-Au was thereby less than that needed for the formation of Ge(335)-Au domains on the Ge(557) substrate. Therefore the Au coverage of the Ge(335)-Au terraces is likely to be lower than the one monolayer Au coverage of the Ge(111)-Au surface [41]. A submonolayer coverage would also be consistent with the Au coverages of the Si(*hkk*)-Au surfaces [6]. Large areas up to 100 nm in width covered with regular Ge(335)-Au steps can be seen in STM images [see Fig. 4(b)]. Detailed images also show the  $\times 3$  superstructure observed with LEED [green dots in Fig. 4(c)] in small sections parallel to the step edge direction. The chain featuring the  $\times 3$  superstructure shows inverted intensities between the occupied and unoccupied states. This is

comparable to the well understood Si(335)-Au surface which also exhibits inverted intensities at its Si HC step edge [see Fig. 4(c) (on the right side)] [40]. Krawiec *et al.* [42] attributed the bias-dependent intensity inversion to alternating empty and fully occupied dangling bonds of the Si step edge atoms. Another similarity of Si(335)-Au and Ge(335)-Au, besides the intensity inversion, is the display of only one type of chainlike structure in STM images. Therefore, one may infer a similar atomic structure for both surfaces. The Si(335)-Au structure model [6,43] is comprised of a Si honeycomb step edge with a single Au chain on each terrace, as depicted in analogy for Ge(335)-Au in Fig. 4(d). The bias-dependent  $\times 3$  superstructure along the Ge(553)-Au step edge may be related to an alternating electron occupancy of the step edge dangling bonds, similar to what is found for Si(335)-Au [42].

#### IV. DISCUSSION AND CONCLUSIONS

In summary, we report on the successful experimental realization of three different Ge(*hkk*)-Au surfaces. In the course of the Ge(557) substrate preparation, we have found the bare Ge(223) surface to be exceptionally stable, showing a well-ordered surface reconstruction with three different structural elements, namely the paired protrusions, spades, and butterflies. Upon Au adsorption, certain bare Ge(*hkk*) surfaces refacet and change their surface orientation, namely (553) to (221)-Au and (223) to either (335)-Au or (557)-Au. The misalignments between the different orientations of the bare substrate and refaceted surfaces are compensated by Ge(111)-Au domains. Each Au-induced Ge(*hkk*) surface shows chainlike 1D structures with superstructures along their step edge direction. The resemblance in STM of Ge(557)-Au and Ge(335)-Au with their Si counterparts is indicative of a possibly similar atomic structure. Based on related atomic structure models of Si(*hkk*)-Au and Ge(111)-M surfaces, a simple atomic structure model is proposed for each Ge(*hkk*)-Au surface. It is likely that Ge(*hkk*)-Au surfaces share their atomic structure motifs with Si(*hkk*)-Au surfaces and consist in general of Ge honeycomb step edges and Au chains. These models should be regarded as a starting point for a thorough investigation of the atomic structure and their energetic stability by DFT or experimentally by, e.g., surface x-ray diffraction (SXR).

Nevertheless, these first STM and LEED measurements of Ge(*hkk*)-Au surfaces show 1D stepped surface reconstructions which strongly resemble those of the related Si(*hkk*)-Au family. This opens up the possibility to investigate the influence of different substrate materials on the electronic properties of these Au-induced nanowire reconstructions without significantly changing the overall atomic structure. Besides the variation of substrate lattice constant and electronic screening the Ge(*hkk*) substrates offer additional advantages. Possessing the smallest terrace width of 1.2 nm among the Si- or Ge(*hkk*)-Au family, Ge(221)-Au provides the possibility to further investigate the evolution of a 1D nanowire surface into the 2D regime with strong interwire coupling. Even more pronounced as for Si(553)-Au and Si(335)-Au [6], the strong 2D interaction should show up as a corrugation of the otherwise straight 1D Fermi surfaces of existing surface bands in angle-resolved photoemission spectroscopy. In addition, the missing lateral shift by  $0.5 a_0$  in the atomic structure of

adjacent terraces on Ge(221)-Au offers a novel template for the magnetic interaction of dangling bond spins in case of a spin-polarized step edge. While the dangling bond spins on Si(553)-Au arrange in a frustrated triangular lattice which is proposed to behave as a spin liquid [44], those on the step edges of Ge(221)-Au could realize a nonfrustrated Heisenberg model square lattice with different magnetic exchange constants parallel and perpendicular to the step edges. The special case of Ge(221)-Au and the similarities of Ge(*hkk*)-Au

surfaces to their Si counterparts will therefore allow insights into the substrates influence on the structural and electronic properties of 1D vicinal Au-induced surfaces.

#### ACKNOWLEDGMENT

This work was supported by Deutsche Forschungsgemeinschaft through Grant FOR 1700 and SFB 1170 “TocoTronics.”

- 
- [1] M. D. Johannes and I. I. Mazin, *Phys. Rev. B* **77**, 165135 (2008).
- [2] T. Giamarchi, *Quantum Physics in One Dimension* (Oxford Science Publications, Oxford, 2003).
- [3] J. Sinova and I. Zutic, *Nat. Mater.* **11**, 368 (2012).
- [4] G. D. Mahan, *Phys. Rev. Lett.* **102**, 016801 (2009).
- [5] M. C. Gallagher, S. Melnik, and D. Mahler, *Phys. Rev. B* **83**, 033302 (2011).
- [6] J. N. Crain, J. L. McChesney, F. Zheng, M. C. Gallagher, P. C. Snijders, M. Bissen, C. Gundelach, S. C. Erwin, and F. J. Himpsel, *Phys. Rev. B* **69**, 125401 (2004).
- [7] J. R. Ahn, P. G. Kang, K. D. Ryang, and H. W. Yeom, *Phys. Rev. Lett.* **95**, 196402 (2005).
- [8] C. Tegenkamp, Z. Kallassy, H. Pfnür, H.-L. Günter, V. Zielasek, and M. Henzler, *Phys. Rev. Lett.* **95**, 176804 (2005).
- [9] U. Krieg, C. Brand, C. Tegenkamp, and H. Pfnür, *J. Phys.: Condens. Matter* **25**, 014013 (2013).
- [10] L. Dudy, J. Aulbach, T. Wagner, J. Schäfer, and R. Claessen, *J. Phys.: Condens. Matter* **29**, 433001 (2017).
- [11] I. Barke, F. Zheng, T. K. Rügheimer, and F. J. Himpsel, *Phys. Rev. Lett.* **97**, 226405 (2006).
- [12] S. C. Erwin and F. J. Himpsel, *Nat. Commun.* **1**, 58 (2010).
- [13] J. Aulbach, J. Schäfer, S. C. Erwin, S. Meyer, C. Loho, J. Settelein, and R. Claessen, *Phys. Rev. Lett.* **111**, 137203 (2013).
- [14] J. Aulbach, S. Erwin, R. Claessen, and J. Schäfer, *Nano Lett.* **16**, 2698 (2016).
- [15] D. Sánchez-Portal, S. Riikonen, and R. M. Martin, *Phys. Rev. Lett.* **93**, 146803 (2004).
- [16] M. Krawiec, *Phys. Rev. B* **81**, 115436 (2010).
- [17] H. Morikawa, K. S. Kim, D. Y. Jung, and H. W. Yeom, *Phys. Rev. B* **76**, 165406 (2007).
- [18] J. A. Lipton-Duffin, A. G. Mark, J. M. MacLeod, and A. B. McLean, *Phys. Rev. B* **77**, 125419 (2008).
- [19] C. Blumenstein, J. Schäfer, S. Mietke, S. Meyer, A. Dollinger, M. Lochner, X. Y. Cui, L. Patthey, R. Matzdorf, and R. Claessen, *Nat. Phys.* **7**, 776 (2011).
- [20] O. Gurlu, O. A. O. Adam, H. J. W. Zandvliet, and B. Poelsema, *Appl. Phys. Lett.* **83**, 4610 (2003).
- [21] R. E. Schlier and H. E. Farnsworth, *J. Chem. Phys.* **30**, 917 (1959).
- [22] P. Palmberg and W. Peria, *Surf. Sci.* **6**, 57 (1967).
- [23] J. Y. Lee and M.-H. Kang, *Phys. Rev. B* **66**, 233301 (2002).
- [24] M. H. von Hoegen, *Z. Kristallogr.* **214**, 684 (1999).
- [25] Y. Margoninski and L. Feinstein, *Surf. Sci.* **23**, 458 (1970).
- [26] P. Höpfner, J. Schäfer, A. Fleszar, J. H. Dil, B. Slomski, F. Meier, C. Loho, C. Blumenstein, L. Patthey, W. Hanke *et al.*, *Phys. Rev. Lett.* **108**, 186801 (2012).
- [27] G. Somorjai and M. V. Hove, *Prog. Surf. Sci.* **30**, 201 (1989).
- [28] M. Czubanowski, A. Schuster, S. Akbari, H. Pfnür, and C. Tegenkamp, *New J. Phys.* **9**, 338 (2007).
- [29] C. H. Mullet and S. Chiang, *J. Vac. Sci. Technol. A* **31**, 020602 (2013).
- [30] M. Kopciuszynski, P. Dyniec, R. Zdyb, and M. Jałochowski, *Phys. Rev. B* **91**, 235420 (2015).
- [31] J. Schäfer, S. C. Erwin, M. Hansmann, Z. Song, E. Rotenberg, S. D. Kevan, C. S. Hellberg, and K. Horn, *Phys. Rev. B* **67**, 085411 (2003).
- [32] S. I. Bozhko, A. M. Ionov, and A. N. Chaika, *Semiconductors* **49**, 753 (2015).
- [33] A. Chaika, D. Fokin, S. Bozhko, A. Ionov, F. Debontridder, T. Cren, and D. Roditchev, *Surf. Sci.* **603**, 752 (2009).
- [34] I. Barke, F. Zheng, S. Bockenhauer, K. Sell, V. v. Oeynhausen, K. H. Meiwes-Broer, S. C. Erwin, and F. J. Himpsel, *Phys. Rev. B* **79**, 155301 (2009).
- [35] M. Sauter, R. Hoffmann, C. Sürgers, and H. v. Löhneysen, *Phys. Rev. B* **89**, 075406 (2014).
- [36] I. K. Robinson, P. A. Bennett, and F. J. Himpsel, *Phys. Rev. Lett.* **88**, 096104 (2002).
- [37] D. Sánchez-Portal and R. M. Martin, *Surf. Sci.* **532-535**, 655 (2003).
- [38] H. W. Yeom, J. R. Ahn, H. S. Yoon, I.-W. Lyo, H. Jeong, and S. Jeong, *Phys. Rev. B* **72**, 035323 (2005).
- [39] J. R. Ahn, H. W. Yeom, H. S. Yoon, and I.-W. Lyo, *Phys. Rev. Lett.* **91**, 196403 (2003).
- [40] M. Krawiec, T. Kwapiński, and M. Jałochowski, *Phys. Status Solidi B* **242**, 332 (2005).
- [41] P. B. Howes, C. Norris, M. S. Finney, E. Vlieg, and R. G. van Silfhout, *Phys. Rev. B* **48**, 1632 (1993).
- [42] M. Krawiec, *Surf. Sci.* **609**, 44 (2013).
- [43] M. Krawiec, *Appl. Surf. Sci.* **254**, 4318 (2008).
- [44] B. Hafke, T. Frigge, T. Witte, B. Krenzer, J. Aulbach, J. Schäfer, R. Claessen, S. C. Erwin, and M. Horn-von Hoegen, *Phys. Rev. B* **94**, 161403(R) (2016).